International Journal of Computer Applications (0975 - 8887)
Volume 187 - No.112, June 2026

A Low-Light Color Image Enhancement Model with a Trainable Intuitionistic Fuzzy Generator

Gayathri Ramesh
Department of Applied Mathematics
Bharathiar University
Coimbatore 641046, India

Dhanalakshmi Palanisami
Department of Applied Mathematics
Bharathiar University
Coimbatore 641046, India

Gokulakrishnan Dhamotharan
Department of Applied Mathematics
Bharathiar University
Coimbatore 641046, India

Nandhini Mohan
Department of Applied Mathematics
Bharathiar University
Coimbatore 641046, India

ABSTRACT

Low-light image enhancement techniques enable better visual quality by showing hidden structural details that become visible through their application. Traditional contrast enhancement methods that improve visibility create challenges because they alter fundamental image structures while increasing noise levels. The trainable Intuitionistic Fuzzy Generator (TIFG) serves as solution for this particular situation because it improves the quality of dimly illuminated images. The proposed technique establishes an intuitionistic fuzzy set framework to model uncertainty about low-light conditions through a specific improvement process. Unlike traditional fuzzy generators with fixed complements, TIFG employs trainable membership, non-membership, and hesitation functions, allowing adaptive learning of enhancement parameters. To provide stability across a range of illumination levels, these parameters are tuned using the Adam optimizer and a custom loss function. The process uses Contrast Limited Adaptive Histogram Equalization (CLAHE) to achieve two objectives that include reducing noise amplification and improving local contrast. The TIFG+CLAHE method establishes its superior visual quality and quantitative performance through its experiments conducted on the Low-Light (LoLI), ExDark, and MIT-5K datasets that show its strength against traditional enhancement methods. Therefore, the results demonstrate that the TIFG+CLAHE method is an effective framework that adapts to different image enhancement scenarios.

Keywords

Low-light color image enhancement, intuitionistic fuzzy sets, trainable intuitionistic fuzzy generator, contrast enhancement.

1. INTRODUCTION

Images are often captured in sub-optimal lighting environments, due to issues like backlighting, uneven illumination, or low-light environments. These problems develop because of two required conditions which include inadequate lighting conditions and short duration of light exposure. The quality of captured images decreases because of their current state and this leads to poor presentation of critical content. The image quality degradation affects human visual perception while it also hinders advanced computer vision systems from performing object tracking and recognition and detection tasks [1]. Image processing acts as a core component of computer vision and digital signal processing because it enables users to handle, assess, and understand visual material for the purpose of discovering relevant content. The image enhancement field has developed into a primary research area because medical imaging, surveillance, remote sensing and autonomous systems require clear and high-quality visuals. In order to make images easier for both humans and machines to analyze, image enhancement aims to minimize undesirable elements while highlighting crucial ones. Researchers have developed a variety of enhancement techniques, ranging from more sophisticated approaches that involve fuzzy logic, machine learning, and deep learning to more conventional approaches like spatial filtering and histogram equalization (HE). Accordingly, recent research has focused on the development of robust and adaptive image enhancement techniques that preserve perceptual quality under low-light and uneven illumination conditions. The rapid advancement of computer vision and pattern recognition has led to numerous approaches to improve low-light images [2], [3]. Because it can accurately represent uncertainty and imprecision, fuzzy set theory has become one of these methods most promising frameworks for image enhancement. Since its initial introduction by Zadeh in 1965 [4], fuzzy set theory has been widely applied across various domains, with notable success in image processing applications. Classical fuzzy sets can only express degrees of support and opposition without hesitation. Atanassov [5] developed intuitionistic fuzzy sets as a solution to this problem that enhanced fuzzy sets with three additional membership degrees. The improved framework allows better uncertainty modeling through its extra membership and non-membership and hesitation degrees. In 1996, Burillo and Bustince [6] further advanced this theory by formally defining entropy within the context of IFSs. Hanmandlu and Jha [7] presented a global contrast enhancement method that

uses a fuzzification component together with an intensification control parameter. A quick approach that combines fuzzy logic and HE was created by Raju and Nair [8] to convert RGB photos into the HSV color space while maintaining the original color information. Similarly, Kaur and Sidhu [9] proposed an efficient fuzzy and HE-based method that demonstrated effectiveness in diverse applications, including underwater imaging, remote sensing, and medical image enhancement. The low contrast, low brightness, and sensor noise that these images usually exhibit present serious obstacles to human vision as well as to later computer vision tasks such as object detection and segmentation of images. Over the past several decades, HE and fuzzy logic-based techniques have significantly enhanced images captured in low light. Image quality and visual attractiveness have been improved through the development of HE-based enhancement methods for images [10]-[15]. Jiang et al. [16] proposed a method which enables users to select proper histogram profiles by using image intensity adjustments that keep output brightness near the original image brightness level. Since most HE variants are based on global processing, they are limited in handling local illumination variations and often fail to address inconsistencies caused by non-uniform lighting conditions. Despite the advancements of global processing techniques, handling variations in non-uniformly illuminated images remains a challenge. Adaptive Histogram Equalization (AHE) was created by Puer et al. [17] as a solution to their problem because it improves local contrast by processing small image areas called tiles. Bilinear interpolation is employed to reduce artificial boundaries between adjacent tiles. AHE shows effective performance but increases noise effects especially in areas with uniform texture. The development of CLAHE created a solution to this problem by introducing a clip limit which prevents excessive enhancement. Reza [18] introduced CLAHE as a system level implementation in 2003 which enabled its use in Very-Large-Scale Integration (VLSI) systems. While Chang et al. [19] created an automated CLAHE system to boost image contrast, Yadav et al. [20] applied CLAHE for real-time video enhancement. Chaira [41],[42] proposed a novel image enhancement method for mammogram images using Atanassov's IFS theory. Jebadass and Balasubramaniam [23],[24] established their method that combines histogram equalization with intuitionistic fuzzy images (IFI). In order to enhance method performance, they developed an improved enhancement technique that merged CLAHE with interval-valued intuitionistic fuzzy images (IVIFI). Image enhancement techniques are classified into two primary groups: traditional approaches and learning-based methods. Conventional techniques, including HE, AHE, CLAHE, and Gamma correction, can enhance visual quality under specific conditions. The methods become ineffective because they cannot deal with complex low-light situations and they do not demonstrate strength in new situations. The research field introduced deep learning-based low-light enhancement techniques were proposed [25]-[30], and numerous innovative solutions surfaced that used frameworks for learning that is supervised, unsupervised, and reinforcement learning techniques to model illumination characteristics more effectively. Learning-based methods showed better adaptability and visual performance than traditional methods according to the study results. The Challenges in improving low light picture quality: There are a number of variables that make the process of enhancing low-light images inherently difficult. First, brightness improvement often leads to noise amplification, especially in dark regions. Second, the process of preserving structural and textural details becomes difficult because underenhancement hides vital information and over-enhancement creates visual artifacts. Third, the conventional IFGs limit their capacity with fixed parameters that restrict their ability to function in different lighting conditions. Finally, the main challenge of the system involves maintaining fuzzy consistency between membership and non-membership and hesitation components while the model needs to work effectively in actual environments, particularly in varying lighting and scene complexities that can affect performance. The existing problems demonstrate the requirement for adaptive intelligent enhancement systems that will automatically control the three main functions of brightness enhancement and noise reduction and detail preservation.

The primary motivations of the proposed study are described in the following summary: The combination of insufficient lighting and low-light conditions results in image capture that loses structural details and color accuracy while displaying reduced contrast and increased noise levels. Critical images, including medical scans, surveillance footage, and remote sensing data, suffer from detail loss and false detection problems when brightness adjustment methods or noise reduction methods are implemented incorrectly. The research problem of creating a reliable system to improve pictures taken in low light is still unresolved. Fuzzy sets and their extra features have become widely used in image-enhancing processes because of their capacity to manage ambiguous and inaccurate data. The Intuitionistic Fuzzy Generator (IFG) maps pixel intensities into membership, non-membership, and hesitation degrees, effectively representing illumination ambiguity. The application of IFGs has shown successful results with low-light images through the implementation of Yager, Sugeno, and Chaira methods. The present study explores improved intuitionistic fuzzy formulations to enhance low-light images based on these observations. This recent advancement raises several important research questions.

(a) Is it possible to design a new IFG that more accurately models illumination uncertainty in low-light images?

(b) How can an IFG be made more powerful than existing formulations for enhancing severely underexposed images?

(c) Is it feasible to create a framework for adaptive low-light picture enhancement that consistently improves contrast, brightness, and structural features in a variety of lighting scenarios?

Existing techniques for enhancing low-light images need mathematical approach to achieve better results because they currently face specific limitations. The research study presents its main contributions according to the following summary of main findings.

(1) **Design a new IFG**: To design an IFG for an accurate pixel-wise fuzzy representation.

(2) **Develop a trainable framework**: To construct a TIFG that can adaptively learn the membership, non-membership, and hesitation degrees for each pixel.

(3) **Enhance image quality**: To optimize the enhancement process through a composite loss function integrating reconstruction accuracy and fuzzy constraint terms, and to improve low-light image visibility by enhancing brightness, contrast, and structural clarity.

(4) **Integration with benchmark methods**: CLAHE is incorporated within the proposed framework to further refine enhancement performance.

(5) **Comprehensive evaluation**: The proposed method was assessed through a complete evaluation process that compared its performance against existing techniques including HE, AHE, CLAHE, Gamma Correction, and IFI, on benchmark low-light datasets through standard quantitative image quality metrics.

The remaining portion of the paper is organized as follows. In Section 2, the basic concepts are presented. The proposed

TIFG+CLAHE framework for improving low-light images is explained in Section 3. The datasets, evaluation metrics, and experimental setup are described in Section 4. The qualitative and quantitative results are covered in Section 5, and Section 6 provides a summary of the contributions and future study paths.

2. FUNDAMENTAL CONCEPTS

The section outlines basic concepts that establish the theoretical framework for the current study and allow for complete comprehension of the proposed methods that will be applied.

2.1 Fuzzy Sets

Let us assume that U is a non-empty the universal set [31]. A fuzzy set X over U has the following definition:

$$X = \{(u, \mu_X(u)) \mid u \in U\}, \tag{1}$$

where $\mu_X(u) : U \to [0, 1]$ indicates the degree of corresponding membership of the component u in the set X.

2.2 Intuitionistic Fuzzy Sets (IFSs)

As a generalization technique for fuzzy sets, Atanassov developed IFSs, which allows different membership levels to be assigned to each element [32]. The definition of an IFS $\tilde{X}$ that applies to the universal set U is expressed as

$$\tilde{X} = \{(u, \mu_{\tilde{X}}(u), \vartheta_{\tilde{X}}(u)) \mid u \in U\}, \tag{2}$$

where $\mu_{\tilde{X}}(u), \vartheta_{\tilde{X}}(u) \in [0, 1]$ denotes the degrees of membership and non-membership, respectively, according to the condition

$$0 \leq \mu_{\tilde{X}}(u) + \vartheta_{\tilde{X}}(u) \leq 1. \tag{3}$$

When $\vartheta_{\tilde{X}}(u) = 1 - \mu_{\tilde{X}}(u)$, the IFS reduces to a standard fuzzy set.
The definition of the hesitation degree $\pi_{\tilde{X}}(u)$, which represents the uncertainty related to element u, is

$$\pi_{\tilde{X}}(u) = 1 - \mu_{\tilde{X}}(u) - \vartheta_{\tilde{X}}(u), \quad 0 \leq \pi_{\tilde{X}}(u) \leq 1, \tag{4}$$

Accordingly, the effective membership of u lies within the interval $[\mu_{\tilde{X}}(u), \mu_{\tilde{X}}(u) + \pi_{\tilde{X}}(u)]$.

2.3 Concept of IFG for Image Enhancement

A mapping $c : [0, 1] \to [0, 1]$ is called a fuzzy complement. However, constructing an IFS as,

$$\tilde{X} = \{(u, \mu_X(u), c(\mu_X(u))) \mid u \in U\} \tag{5}$$

does not always constitute a valid IFS, since the condition $\mu_X(u) + c(\mu_X(u)) \leq 1$ may be violated. Such violations lead to a negative hesitation degree $\pi_{\tilde{X}}(u) < 0$, which compromises the theoretical consistency of the intuitionistic fuzzy framework.
For instance, the Yager class of fuzzy complements [33] has the following definition:

$$c(\mu_X(u)) = \left(1 - (\mu_X(u))^b\right)^{1/b}, \quad 0 < b < 1, \tag{6}$$

and Sugeno class [34] is given by

$$c(\mu_X(u)) = \frac{1 - \mu_X(u)}{1 + b\,\mu_X(u)}, \quad b \geq 0. \tag{7}$$

Although widely adopted, these complement functions may produce non-membership values that violate the fundamental intuitionistic fuzzy constraint, leading to negative hesitation degrees.

To overcome this limitation, an IFG is introduced as a constrained fuzzy complement that ensures the validity of intuitionistic fuzzy representations. An IFG provides a systematic mechanism for deriving the degree of non-membership from the degree of membership, such that the fundamental condition

$$0 \leq \mu_{\tilde{X}}(u) + \nu_{\tilde{X}}(u) \leq 1, \quad \forall u \in U. \tag{8}$$

is always satisfied, where $\mu_{\tilde{X}}(u), \nu_{\tilde{X}}(u)$, and $\pi_{\tilde{X}}(u) = 1 - \mu_{\tilde{X}}(u) - \nu_{\tilde{X}}(u)$ represent the degrees of membership, non-membership, and hesitation, respectively. A function in formal terms,

$$Q : A \to [0, 1] \tag{9}$$

is considered an IFG if it satisfies $Q(a) \leq 1-a, \quad \forall a \in [0, 1]$, with the boundary constraints $Q(0) = 1, \quad Q(1) = 0$, where A denotes the universal set and $a \in A$. Typically, an IFG is selected as a continuous and monotonic function that uses $\nu_{\tilde{X}}(u) = Q(\mu_{\tilde{X}}(u))$ to establish the relationship between the degrees of membership and non-membership. These constraints ensure that the hesitation degree $\pi_{\tilde{X}}(u) = 1 - \mu_{\tilde{X}}(u) - Q(\mu_{\tilde{X}}(u))$ remains non-negative. Moreover, the generator is required to be involutive, i.e.,

$$Q(Q(\mu_{\tilde{X}}(u))) = \mu_{\tilde{X}}(u), \tag{10}$$

making certain that membership and non-membership functions are symmetrical.
The establishment of an accurate IFG design becomes crucial for image enhancement tasks that operate in low-light and complicated lighting conditions. Accordingly, the IFG functions as a fundamental generating mechanism that regulates the distribution of non membership and hesitation degrees within the intuitionistic fuzzy representation. A well-designed IFG enables effective enhancement by sustaining structural details in darker regions while preserving overall contrast and visual uniformity across the image.

2.4 Contrast Limited Adaptive Histogram Equalization (CLAHE)

In CLAHE, the equivalent transformation function is obtained by applying an expansion function to local neighborhoods. Unlike AHE, CLAHE controls contrast enhancement through its method of histogram peak restriction that prevents over-enhancement and excessive intensity changes [35]. The CLAHE technique is carried out as shown in Algorithm 2.4

Algorithm 1: CLAHE for Low-Light Color Image Enhancement

Input: Image I, tile size $N_x^{cr} \times N_y^{cr}$, gray levels N_{gray}, clip limit N_{clip}

Output: Enhanced image I_{enh}

(1) Divide I into non-overlapping tiles T_k.
(2) For each tile T_k:
   (a) Compute histogram $H_T(i)$.
   (b) Compute clip limit:

$$N_{cl} = N_{clip} \cdot \frac{N_x^{cr} N_y^{cr}}{N_{gray}}$$

   (c) Clip histogram and accumulate excess pixels.
   (d) Redistribute clipped pixels uniformly.
   (e) Normalize histogram:

$$P_T(i) = \frac{H_T(i)}{\sum H_T(i)}$$

(f) Compute CDF:

$$CDF_T(i) = \sum_{j=0}^{i} P_T(j)$$

(g) Map pixels:

$$I_{enh}(x,y) = (N_{gray} - 1)\, CDF_T(I(x,y))$$

(3) Merge tiles using bilinear interpolation.

(4) Return I_{enh}.

3. METHODOLOGY

This section shows the formulation of the trainable intuitionistic fuzzy image representation was built through the development of the generator parameter γ, the hesitancy degree, and the defuzzification process to provide a clear observation of the suggested method. The primary objective of the study is to use these theoretical concepts to develop an effective framework for image enhancement. Using the suggested TIFG, images taken in low light levels are adaptively improved. The complete workflow of the proposed method, including the intermediate outcomes that are obtained at each point of the processing stage, is illustrated in figure 1 to facilitate better visualization and analysis of the model behavior.

3.1 Fuzzy Image (FI)

Let I denote the original image, in which every pixel's intensity value lies within the range $[0, 255]$. The fuzzy representation of the crisp image develops through a membership function that uses normalization to process the image [36]. This process maps each pixel intensity to a corresponding membership value within the interval $[0, 1]$. A set of fuzzy singletons can be used to represent a digital image I of size $U \times V$. The fuzzification of the image is defined as 11:

$$\mu(I(u,v)) = \frac{I_{uv} - I_{\min}}{I_{\max} - I_{\min}}, \quad 1 \le u \le U,\ 1 \le v \le V, \qquad (11)$$

where $I_{\max}$ and $I_{\min}$ are the highest and lowest value of gray levels in the image, respectively, and I_{uv} represents the value of pixels.

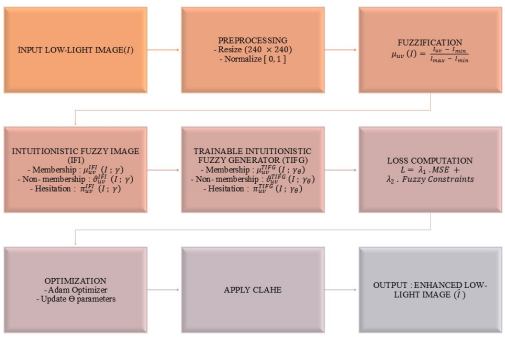

Fig. 1. Workflow of the proposed TIFG-Based Enhancement method

3.2 Formulation of an IFG

The definition of a fuzzy complementary function is necessary for the establishment of an IFG. However, their formulation strongly depends on the use of an IFG [37]. This subsection introduces an IFG formulation that specifically solves problems that occur during low-light image enhancement.
To construct a new fuzzy complement, an increasing function H is employed such that $H(0) = 0$. Let $Q : [0,1] \to [0,1]$ denote the involutive fuzzy complement function. The general expression of an IFG is defined by:

$$Q(\mu(a)) = H^{-1}\big[H(1) - H(\mu(a))\big] \qquad (12)$$

where H is defined as an increasing and continuous function,

$$H(\mu(a)) = \frac{1}{\gamma - 1} \log\Big[1 + \mu(a)(\gamma - 1)\Big] \qquad (13)$$

with $\gamma > 1$. For simplicity, let $x = \mu(a)$, Then, the equaion 13 can be rewritten as:

$$H(x) = \frac{1}{\gamma - 1} \log\Big[1 + x(\gamma - 1)\Big] \qquad (14)$$

such that $H(0) = 0$ and $H(1) = \frac{1}{\gamma - 1} \log \gamma$, where γ is a constant. The corresponding inverse function is derived as:

$$H^{-1}(x) = \frac{e^{x(\gamma-1)} - 1}{\gamma - 1} \qquad (15)$$

Consequently, the complement function 12 becomes ,

$$\begin{aligned} Q(x) &= H^{-1}\left[\frac{1}{\gamma - 1}\log(1) - \frac{1}{\gamma - 1}\log(1 + x(\gamma - 1))\right] \\ &= H^{-1}\left[\frac{1}{\gamma - 1}\log\left(\frac{\gamma}{1 + x(\gamma - 1)}\right)\right] \end{aligned} \qquad (16)$$

Finally, solving this equation gives the fuzzy complement function in closed form:

$$Q(x) = \frac{1 - x}{1 + x(\gamma - 1)} \qquad (17)$$

Therefore, the membership function $\mu(a)$ can be used to express the developed IFG as follows:

$$Q(\mu(a)) = \frac{1 - \mu(a)}{1 + \mu(a)(\gamma - 1)} \qquad (18)$$

It can be verified that equation 18 satisfies the condition $Q(\mu(a)) \le 1 - \mu(a)$ for all γ and $\mu(a) \in [0,1]$. Moreover, it meets all the required properties of an IFG, making it a suitable formulation for improving low-light images.

3.3 IFG-Based Approach for Low Light Image Enhancement

As discussed earlier, image augmentation is a crucial component of low-light image processing because inadequate lighting conditions lead to diminished visibility and reduced contrast and missing vital information. The hidden elements need to be enhanced through effective contrast enhancement because they enable correct visual interpretation which supports the later analysis process. At the same time, the enhancement process must be carefully controlled to prevent excessive brightening or darkening, since over-

or under-enhancement can distort visual content and decreases image authenticity. Therefore, this subsection concentrates on image enhancement using the developed IFG.
Let I be the original image of size $U \times V$. The first step is to fuzzify the source image using equation 11 respectively, and then use the developed IFG defined in 18 to turn the fuzzified image into an IFI. The IFI's membership function is expressed as follows:

$$\begin{aligned} \mu_{uv}^{IFI}(I;\gamma) &= 1 - \frac{1-\mu_{uv}(I)}{1+\mu_{uv}(I)(\gamma-1)} \\ &= \frac{\mu_{uv}(I)\,\gamma}{1+\mu_{uv}(I)(\gamma-1)} \end{aligned} \tag{19}$$

The corresponding non-membership function is derived as:

$$\nu_{uv}^{IFI}(I;\gamma) = P(\mu_{uv}^{IFI}(I;\gamma)) = \frac{1-\mu_{uv}^{IFI}(I)}{1+\mu_{uv}^{IFI}(I)(\gamma^2-1)} \tag{20}$$

Meanwhile, the hesitation degree is calculated as:

$$\pi_{uv}^{IFI}(I;\gamma) = 1 - \mu_{uv}^{IFI}(I;\gamma) - \nu_{uv}^{IFI}(I;\gamma) \tag{21}$$

3.4 Construction of TIFG

While the proposed IFG enhances low-light images by improving contrast and preserving details, its performance can still be limited by the fixed parameter γ. The complete range of low-light image characteristics can be observed through different light conditions which display distinct noise patterns and specific scene structures. A static formulation will not deliver optimal enhancement results throughout all situations. The TIFG concept establishes the framework to optimize membership parameters through adaptive optimization of non-membership and hesitation degree parameters.
The central idea of TIFG is to parameterize the IFG so that it can be enable data-driven learning methods to adjust their operation. In this method, learnable parameters that can be adjusted for specific improvement, such as maximizing entropy, fuzzy constraints, or perceptual quality, are used instead of fixed membership, non-membership, and hesitation functions.
The fuzzified trainable membership degree at pixel location (u, v) is generalized as:

$$\mu_{uv}^{TIFG}(I;\gamma_\theta) = \frac{\mu_{uv}(I)\cdot\gamma_\theta}{1+\mu_{uv}(I)(\gamma_\theta-1)}, \tag{22}$$

where $\mu_{uv}(I)$ is the normalized fuzzification defined in equation 11, and γ_θ is a trainable parameter (or a set of parameters) learned from data rather than being manually chosen.
The trainable non-membership degree is defined as a parameterized complement of the membership function:

$$\nu_{uv}^{TIFG}(I;\gamma_\theta) = \frac{1-\mu_{uv}^{TIFG}(I;\gamma_\theta)}{1+\mu_{uv}^{TIFG}(I;\gamma_\theta)(\gamma_\theta^2-1)}. \tag{23}$$

This ensures that the non-membership function constantly evolves with the learned membership function while still maintaining the constraints of intuitionistic fuzzy sets.
The trainable hesitation degree, which captures the uncertainty in the intuitionistic fuzzy representation, is computed as:

$$\pi_{uv}^{TIFG}(I;\gamma_\theta) = 1 - \mu_{uv}^{TIFG}(I;\gamma_\theta) - \nu_{uv}^{TIFG}(I;\gamma_\theta). \tag{24}$$

This representation allows the hesitation degree to automatically adjust based on the optimization of γ_θ. Through its trainable parameters the TIFG system achieves better results when processing different low-light image types than static IFG methods. The trainable structure also opens the possibility of integrating deep learning optimization strategies, where the parameters θ can be updated through backpropagation using task-specific loss functions.

3.5 Loss Function for TIFG

The effectiveness of the proposed TIFG depends critically on the optimization of its parameters γ_θ. The design of our composite loss function combines pixel-level fidelity and fuzzy consistency, enabling us to achieve visually improved low-light images while maintaining their structural integrity.

(1) **Reconstruction Loss:** To improve visibility without causing distortions, then use the Mean Squared Error (MSE) between the target image I^t and enhanced image $\hat{I}$:

$$L_{MSE} = \frac{1}{UV}\sum_{u=1}^{U}\sum_{v=1}^{V}\left(\hat{I}_{uv} - I_{uv}^{t}\right)^2. \tag{25}$$

This term enforces pixel-level similarity, ensuring consistency with the original image content.

(2) **Fuzzy Constraint Loss:** Since intuitionistic fuzzy sets must satisfy

$$\mu_{uv}^{TIFG}(I;\gamma_\theta) + \nu_{uv}^{TIFG}(I;\gamma_\theta) + \pi_{uv}^{TIFG}(I;\gamma_\theta) = 1, \tag{26}$$

To reduce departures from this requirement, we implement a fuzzy consistency penalty:

$$L_{fuzzy} = \frac{1}{UV}\sum_{u=1}^{U}\sum_{v=1}^{V}\left|1 - \left(\mu_{uv}^{TIFG} + \nu_{uv}^{TIFG} + \pi_{uv}^{TIFG}\right)\right|. \tag{27}$$

It is preferred that the learned membership, non-membership, and hesitation degrees remain within valid intuitionistic fuzzy bounds.

(3) **Combined Loss:** The two components are combined into a weighted final loss function:

$$L(\gamma_\theta) = \lambda_1 L_{MSE} + \lambda_2 L_{fuzzy}, \tag{28}$$

where λ_1, λ_2 are hyperparameters to balance between reconstruction accuracy and fuzzy constraints. The composite loss function ensures that TIFG fixes the theoretical boundaries of intuitionistic fuzzy sets while it enhances brightness and contrast performance without losing any details.

3.6 Optimization Strategy

The IFG training process needs a specialized optimization technique that can provide both stable convergence results and the ability to function in various low-light environments. The benefits of momentum-based gradient descent are then effectively combined with adaptive learning rate adjustment using the Adam optimizer.
Let $\Theta = \{\mu^{TIFG}, \nu^{TIFG}, \pi^{TIFG}\}$ represent the TIFG parameters. Adam updates Θ by reduces the composite loss function $L(\gamma_\theta)$. The parameter update rule can be expressed as follows:

$$\Theta_{k+1} = \Theta_k - \eta\frac{\hat{m}_k}{\sqrt{\hat{v}_k}+\epsilon}, \tag{29}$$

Here Θ_k denotes the parameter vector at iteration k, η represents the learning rate, $\hat{m}_k$ and $\hat{v}_k$ are the bias-corrected initial- and second-order moment estimations of the gradient, respectively and ϵ is a small constant added to maintain numerical stability.

The estimations for the first and second moments are updated recursively as follows:

$$m_k = \beta_1 m_{k-1} + (1-\beta_1) g_k, \tag{30}$$

$$v_k = \beta_2 v_{k-1} + (1-\beta_2) g_k^2, \tag{31}$$

with bias-correction applied according to:

$$\hat{m}_k = \frac{m_k}{1-\beta_1^k}, \quad \hat{v}_k = \frac{v_k}{1-\beta_2^k}. \tag{32}$$

In this case, the gradient of the loss coefficient with regard to Θ_k is represented by $g_k = \nabla_{\Theta_k} L(\Theta)$, and the moving averages are controlled by exponential decay rates denoted by β_1 and β_2.
Learning rate updates that adjust to each parameter dimension are used in the method to improve convergence speed while reducing the typical oscillation behavior that occurs in non-convex optimization. It proves highly effective for TIFG because its membership, non-membership and hesitation functions exhibit strong non-linearities. As a result, Adam enables TIFG to acquire stable parameter values, generalize well across varying illumination conditions, and consistently produce enhanced outputs.

3.7 Defuzzification

Finally, the reconstructed image $\hat{I}$, the learned intuitionistic fuzzy representation is converted back into the spatial intensity domain. The defuzzification process maps the enhanced fuzzy values are linearly normalized with respect to the image's minimum and maximum intensity values, mapping them to standard pixel intensities. This normalization ensures that the reconstructed image requires all intensity levels in the range $[0, 255]$ by maintaining the relationships between pixel intensities, enhancing visual contrast. The process of defuzzification is defined as

$$\hat{I}_{uv} = \frac{I_{uv} - I_{\min}}{I_{\max} - I_{\min}} \times 255$$

where I_{min} and I_{max} stands for the image's minimum and maximum intensity values, respectively.

3.8 Proposed Algorithm for Image Enhancement using TIFG

The formulation of the TIFG+CLAHE, along with the composite loss and Adam-based optimization methods creates a full framework for enhancing low-light images. This subsection presents the complete algorithm that integrates fuzzification, intuitionistic fuzzy representation, trainable parameter learning until it reaches final defuzzification to produce enhanced outputs. The enhancement process based on the proposed TIFG+CLAHE is summarized in Algorithm 3.8.

Algorithm 2: Proposed TIFG + CLAHE-Based Low-Light Image Enhancement

Input: Low-light image I of size $U \times V$, target image I^t, parameters λ_1, λ_2

Output: Enhanced image $\hat{I}$

(1) **Normalization:** Convert intensities to fuzzy domain:

$$\mu_{uv}(I) = \frac{I_{uv} - I_{\min}}{I_{\max} - I_{\min}}$$

(2) **Intuitionistic Fuzzy Mapping:** Generate IF components:

$$\mu_{uv}^{IFI}, \quad \nu_{uv}^{IFI}, \quad \pi_{uv}^{IFI}$$

(3) **TIFG Transformation:** Learn adaptive fuzzy representation:

$$\mu_{uv}^{TIFG}, \quad \nu_{uv}^{TIFG}, \quad \pi_{uv}^{TIFG}$$

(4) **Loss Computation:**

$$L(\theta) = \lambda_1 L_{MSE} + \lambda_2 L_{fuzzy}$$

(5) **Optimization:** Update parameters θ using Adam optimizer until convergence.

(6) **Defuzzification:** Reconstruct image:

$$\hat{I}_{uv} = \frac{I_{uv} - I_{\min}}{I_{\max} - I_{\min}} \times 255$$

(7) **CLAHE Enhancement:** Apply CLAHE to $\hat{I}$ for local contrast improvement.

(8) **Output:** Return final enhanced image $\hat{I}$.

4. EXPERIMENTAL ANALYSIS

This section provides a detailed description of the experimental setup used in this part, including the dataset characteristics, implementation settings, and evaluation methods. Furthermore, the quantitative performance metrics employed are outlined, highlighting their role in objectively assessing and validating the efficacy of the proposed framework in contrast to comparison with existing benchmark methods. The proposed TIFG-based image enhancement model was implemented and evaluated through Google Colab environment, utilizing its cloud GPU resources to support fast training and testing processes. The input low-light images were resized to 240×240 pixel dimensions while the images were normalized to display values between 0 and 1. The training and validation processes used 50 epochs, a batch size of 4, and 240×240 pixel input resolution. With a learning rate of 0.001 and moment estimate of $\beta_1 = 0.9, \beta_2 = 0.999$, the Adam optimizer was used. The composite loss function found in the equation 28 was used to optimize the network. For the reconstruction loss and the fuzzy constraint loss, the weighting coefficients were empirically determined to be $\lambda_1 = 1.0$ and $\lambda_2 = 0.1$. This arrangement successfully balanced adherence to intuitionistic fuzzy requirements with improvement performance.

4.1 Datasets

Experiments were carried out on three benchmark low-light image datasets to evaluate the robustness and generalization capability of the proposed model.

(a) LoLI-Street Dataset: The LoLI dataset [38] contains paired low-light and normal-light images and is widely used for training and evaluating low-light image enhancement methods.

(b) ExDark Dataset: The ExDark dataset [39] consists of real-world images captured under various extreme low-light conditions, providing a challenging benchmark for assessing enhancement performance in dark environments.

(c) MIT-5K Dataset: The MIT-5K dataset [40] contains diverse natural images with professionally enhanced reference images, enabling the evaluation of image enhancement quality across different scene types and illumination conditions.

Before training and testing, every image was preprocessed and converted to RGB. Using these three datasets together also helps make sure the proposed framework is evaluated in a comprehensive way under multiple low-light imaging scenarios, even when the input looks quite different from each other.

4.2 Preprocessing

All images were resized to $240 \times 240 \times 3$ dimensions to achieve consistent input size requirements and to establish stable mini-batch development and to optimize GPU memory consumption while maintaining core structure information. The model evaluation process used complete resolution images to test system reliability while stopping scale-dependent faults from appearing. The pixel values were first changed into floating-point format before being converted to the range of $[0, 1]$. The pretrained encoders required extra ImageNet-based normalization was applied to ensure feature compatibility.

4.3 Evaluation metrics

The effectiveness of the TIFG+CLAHE method was assessed using a combination of quantitative measures and perceptual quality metrics. To ensure fair comparison with existing approaches, standard image quality metrics were employed:

(1) **Mean Squared Error (MSE):** The MSE measures the average squared intensity difference between the enhanced image $\hat{I}$ and the target image I^t. Lower MSE indicates better reconstruction accuracy:

$$MSE = \frac{1}{UV}\sum_{u=1}^{U}\sum_{v=1}^{V}(\hat{I}_{uv} - I^t_{uv})^2 \tag{33}$$

(2) **Peak Signal-to-Noise Ratio (PSNR):** In the context of the dynamic range of pixel intensities, PSNR assesses the overall enhancement fidelity:

$$PSNR = 10\log_{10}\left(\frac{L^2}{MSE}\right) \tag{34}$$

(3) **Structural Similarity Index (SSIM):** To measure the perceptual similarity between two images, SSIM is used. In this work, the similarity between the target image I^t and the enhanced image $\hat{I}$ is assessed using SSIM. It is computed as follows:

$$SSIM(\hat{I}, I^t) = \frac{(2\mu_{\hat{I}}\mu_{I^t} + C_1)(2\sigma_{\hat{I},I^t} + C_2)}{(\mu^2_{\hat{I}} + \mu^2_{I^t} + C_1)(\sigma^2_{\hat{I}} + \sigma^2_{I^t} + C_2)} \tag{35}$$

where $\mu_{\hat{I}}, \mu_{I^t}$ = mean intensity of enhanced and target images ,
$\sigma^2_{\hat{I}}, \sigma^2_{I^t}$ = variances of enhanced and target images, and
$\sigma_{\hat{I},I^t}$ = covariance between enhanced and target images,
$C_1 = (K_1 L)^2, C_2 = (K_2 L)^2, K_1 = 0.01, K_2 = 0.03$

(4) **Absolute Mean Brightness Error(AMBE):** The difference in absolute terms between the mean intensity values for the target image I^t and its enhanced image $\hat{I}$ is measured by AMBE [41]. In relation to the target image, a lower AMBE value denotes improved brightness preservation and increased visual fidelity.

$$AMBE = |\mu(I^t) - \mu(\hat{I})| \tag{36}$$

where the mean brightness of the target image is represented by $\mu(I^t)$ and the enhanced image by $\mu(\hat{I})$, respectively.

(5) **Contrast Improvement Index(CII):** Contrast is quantified using the standard deviation of pixel intensity values [42]. A CII value closer to 1 indicates a successful improvement in contrast.

$$CII = \frac{C(I^t)}{C(\hat{I})} \tag{37}$$

where $C(I^t)$ and $C(\hat{I})$ denote the contrast values of the target image and the enhanced image, respectively.

4.4 Training setup

The low-light image improvement model implemented in the proposed approach was carried out in TensorFlow and trained using publicly available low-light datasets downloaded through KaggleHub. All preprocessing, training, and evaluation procedures were standardized to ensure reproducibility.

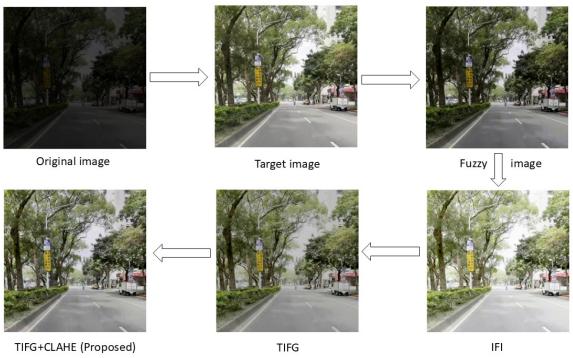

Fig. 2. Simplified flowchart of the proposed technique.

The proposed model was trained with the following configuration as shown in Algorithm 4.4. Futhermore, Figure 2 presents a simplified flowchart of the TIFG+CLAHE enhancement method.

Algorithm 3: Training Procedure for TIFG-Based Low-Light Image Enhancement

Input: Paired low-light and reference images (e.g., LoLI-Street dataset)

Output: Trained TIFG+CLAHE enhancement model

(1) **Load dataset:** Acquire paired training images (I, I^t).

(2) **Preprocessing:**
   (a) Resize images to $240 \times 240 \times 3$.
   (b) Normalize pixel values to $[0, 1]$.

(3) **Initialize training setup:**
   (a) Framework: TensorFlow 2.15 / Python 3.10
   (b) Batch size: 4, Epochs: 50
   (c) Optimizer: Adam ($\beta_1 = 0.9, \beta_2 = 0.999, \epsilon = 10^{-8}$)
   (d) Learning rate: 0.001

(4) **Define loss function:**

$$L(\theta) = \lambda_1 L_{MSE} + \lambda_2 L_{fuzzy}$$

(5) **Training loop:**
   (a) For each epoch:
      i. For each batch (I, I^t):
         A. Fuzzification:

$$\mu_{uv}(I) = \frac{I_{uv} - I_{\min}}{I_{\max} - I_{\min}}$$

         B. IFG mapping: compute $\mu^{IFI}_{uv}(I;\gamma)$, $\nu^{IFI}_{uv}(I;\gamma)$, $\pi^{IFI}_{uv}(I;\gamma)$
         C. TIFG transformation: compute $\mu^{TIFG}_{uv}(I;\gamma_\theta)$, $\nu^{TIFG}_{uv}(I;\gamma_\theta)$, $\pi^{TIFG}_{uv}(I;\gamma_\theta)$
         D. Compute loss $L(\theta)$
         E. Update parameters using Adam optimizer

(6) **Evaluation:**
   (a) Test on full-resolution images
   (b) Compute metrics: PSNR, SSIM, MSE, AMBE, CII

(7) **Output:**
   (a) Save trained model
   (b) Store logs, loss curves, and evaluation results

5. RESULTS AND DISCUSSION

The proposed approach was both trained and tested with the LoLI-Street dataset. All images were resized to 240×240 and divided into training and validation sets. For a fair evaluation, we limited both training and validation samples to 1000 images each using 50 epochs, batch size of 4, and Adam optimizer (lr= 0.001). The training process performed a stable convergence, from the training loss decreasing from 0.3865 to 0.0070 and the validation loss reducing from 0.2175 to 0.0077 over 50 epochs. The results show that both loss metrics dropped continuously, that demonstrates effective learning by the model while preserving its ability to perform accurate mappings from low-light materials to enhanced outputs. Figure 3 demonstrates sample input and target data together with enhanced images that show their corresponding difference maps.

Fig. 3. Sample input, target, and enhanced images with difference maps.

In figure 4, presents the training and validation loss curves for 50 epochs. The plot shows that both training and validation losses decrease steadily which shows that the model achieves stable convergence during the entire training period.

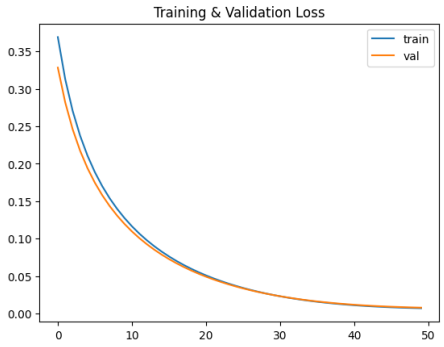

Fig. 4. Training and validation loss curves over 50 epochs.

Enhanced images are given in the figure 5, reveal that dark areas are brightened effectively without creating any visual imperfections. The image preserves its original sharpness for both edges and textures while maintaining a natural appearance throughout the picture. The fuzzy membership formulation enables adaptive enhancement, modifying pixel brightness according to learned membership values to create context-specific contrast enhancements.
In figures 6 and 7, display the original low-light images and enhanced images created by the TIFG+CLAHE method tested on the LoLI-Street dataset.

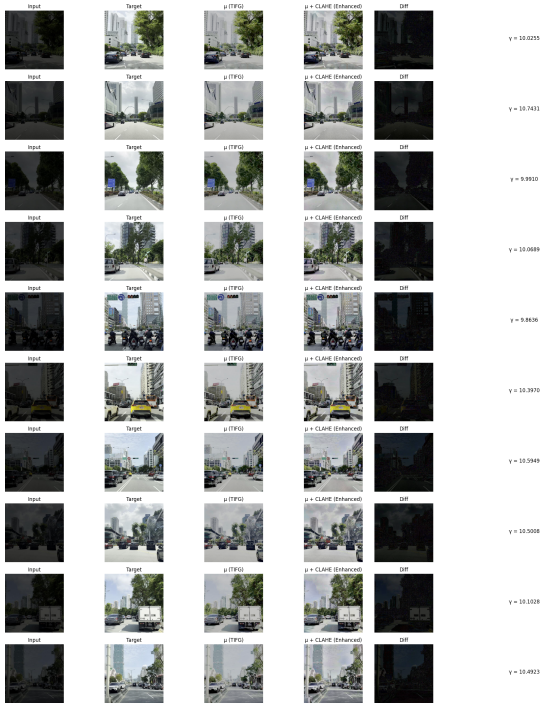

Fig. 5. Source image from LoLI-Street datasets [38] and the output images by using the proposed method

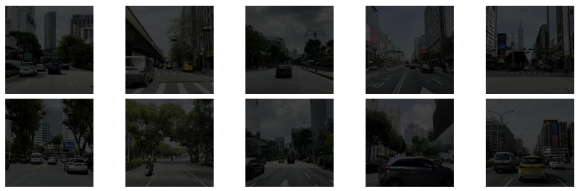

Fig. 6. Original images.

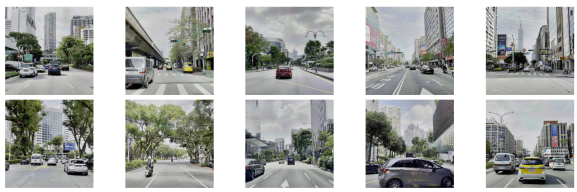

Fig. 7. Enhanced images.

5.1 Performance Measure

This section compares the suggested TIFG+CLAHE model with various conventional image enhancement methods, including HE, AHE, CLAHE, Gamma correction, and IFI. On the LoLI-Street dataset, paired low-light and corresponding normal-light images were used to facilitate objective evaluation. In figure 8 displays the collection of ten image pairs. The first two columns show the original low-light inputs and their ground-truth reference images, while columns 3-9 display the enhancement results obtained using HE, AHE, CLAHE, Gamma correction, IFI, TIFG and the proposed method. Visual inspection makes it clear that the new approach out-

performs existing methods in terms of improvement. The outcomes shown in Table 1 reveal that the proposed approach typically outperforms existing methods in balancing enhancement quality with computing performance.

Table 1. Average Quantitative Performance Comparison of Enhancement Methods

Method	MSE	PSNR	SSIM	AMBE	CII	Time (ms)
HE	**0.00445**	**23.701**	0.8569	0.02565	1.0577	**2.52**
AHE	0.00892	20.534	0.8486	0.08353	1.0210	49.21
CLAHE	0.10393	9.861	0.6100	0.28168	0.5053	4.09
Gamma	0.06434	11.933	0.6888	0.20811	0.4810	4.33
IFI	0.00446	23.681	0.8557	0.02546	1.0592	625.55
TIFG	0.00789	21.053	0.8557	0.04351	0.8289	221.48
TIFG+CLAHE	0.00590	22.329	**0.8830**	**0.02546**	**0.8946**	4.85

(a) **Quantitative Performance**:

The proposed TIFG+CLAHE algorithm was evaluated quantitatively on the LoLI-Street dataset using standard objective metrics such as MSE, PSNR, SSIM, AMBE, and CII. The total test image performance results are displayed in Table 1, shows that the TIFG+CLAHE method maintains an ideal balance between processing speed and image quality. In particular, it yields the highest average SSIM value, indicating superior structural preservation, while maintaining low MSE and competitive PSNR compared to conventional techniques. The AMBE results demonstrate that TIFG+CLAHE effectively maintains the original image brightness, achieving one of the lowest brightness errors among all methods. Furthermore, the CII values obtained by the proposed approach remain close to unity, indicating steady and natural contrast enhancement. As reported in Table 2, the testing of TIFG+CLAHE across all fifteen test images shows it produces lower AMBE values, which establishes its brightness preservation capability. The proposed approach achieves the higest SSIM scores for the majority of images while retaining more structural and textural characteristics, as shown in Table 3. The CII values for fifteen test images that were enhanced using HE, AHE, CLAHE, Gamma correction, IFI, TIFG, and TIFG+CLAHE are shown in Table 4.

Despite the fact that HE and IFI provide relatively higher CII values (especially for Images 4, 14, and 15), these large contrast improvements could be a sign of over-enhancement and possible brightness distribution distortion. Gamma correction and CLAHE result in lower CII values, which indicate less global contrast amplification. The TIFG framework maintains stable CII values across all tested images because it achieves controlled contrast enhancement while preserving structural integrity. The combination of CLAHE with TIFG improves local contrast enhancement while maintaining the same enhancement level. The quantitative results demonstrate that the enhanced method exceeds all traditional histogram-based and fuzzy enhancement methods according to multiple objective metrics.

In figure 11, Combined multi-metric comparison of image enhancement methods. For equitable comparison, performance measures (SSIM, AMBE, CII, and inference time) are standardized to a common scale. Better performance is indicated by higher normalized scores. The proposed TIFG and TIFG+CLAHE methods achieve consistently superior performance across perceptual quality, brightness preservation, contrast improvement, and computational efficiency.

In the ExDark dataset, the proposed TIFG framework was evaluated on ExDark low-light images using MSE, PSNR, SSIM, AMBE, CII, and execution time. Training remained stable, with both training and validation losses decreasing steadily, indicating effective learning without significant overfitting. Experimental results showed that TIFG outperformed HE, AHE, CLAHE, Gamma correction, and IFI in most metrics, achieving the lowest average MSE (0.00025), highest PSNR (38.361 dB), highest SSIM (0.9908), and minimum AMBE (0.01303). Although HE and IFI produced higher CII values, they introduced over-enhancement and distortion, whereas TIFG provided balanced contrast enhancement with natural visual quality. The method also achieved moderate execution time (126.51 ms), making it computationally efficient. In figure 9 presents the visual comparison of enhanced images from the ExDark dataset using different image enhancement techniques. The proposed method produces clearer and naturally enhanced images with improved visibility, balanced contrast, and better preservation of structural details while reducing over-enhancement and brightness distortion.

The fuzzy membership model was further trained on the MIT-5K dataset for 20 epochs, where training and validation losses decreased steadily, demonstrating stable convergence. The lightweight network contained only four trainable parameters. Performance evaluation on five test images showed that the proposed TIFG+CLAHE method achieved the best average MSE (0.01803), highest PSNR (17.913 dB), and lowest AMBE (0.09298), indicating superior reconstruction quality and brightness preservation. While Gamma correction obtained the highest SSIM, TIFG+CLAHE maintained balanced structural preservation and achieved a near-ideal average CII value of 1.0241. Overall, the proposed TIFG and TIFG+CLAHE frameworks ef-

Table 2. Performance measures using AMBE for images shown in Fig. 8

Image	HE	AHE	CLAHE	GAMMA	IFI	TIFG	TIFG+CLAHE
LoLI 1	0.060235	0.082903	0.319351	0.235537	0.059843	0.046501	**0.031635**
LoLI 2	0.024961	0.086466	0.283625	0.213782	0.024882	0.039180	**0.023569**
LoLI 3	0.002463	0.074690	0.282807	0.206729	0.002057	0.041903	**0.021457**
LoLI 4	0.027263	0.087505	0.284505	0.212653	0.027062	0.037178	**0.020789**
LoLI 5	0.023739	0.079886	0.294739	0.215717	0.023607	0.041898	**0.028013**
LoLI 6	0.002392	0.082964	0.285033	0.206905	0.001897	0.042245	**0.022693**
LoLI 7	0.039125	0.083085	0.303841	0.227667	0.038674	0.049907	**0.033611**
LoLI 8	0.028168	0.076852	0.253525	0.186499	0.028263	0.047949	**0.025156**
LoLI 9	0.034954	0.091650	0.291401	0.220420	0.034805	0.039311	**0.025565**
LoLI 10	0.030511	0.102646	0.294666	0.218579	0.030484	0.028423	**0.018083**

Table 3. SSIM values of images shown in Fig. 8

Image	HE	AHE	CLAHE	GAMMA	IFI	TIFG	TIFG+CLAHE
LoLI 1	0.861639	0.853601	0.606448	0.687357	0.858931	0.858474	**0.891746**
LoLI 2	0.888456	0.865377	0.637151	0.689595	0.887737	0.872994	**0.903016**
LoLI 3	0.865355	0.851433	0.611222	0.687677	0.863785	0.854871	**0.873058**
LoLI 4	0.876385	0.869212	0.625947	0.682585	0.876621	0.874357	**0.912282**
LoLI 5	0.859462	0.868555	0.618700	0.704773	0.858626	0.879417	**0.899237**
LoLI 6	0.865876	0.851432	0.608000	0.691472	0.864793	0.857645	**0.873796**
LoLI 7	0.877541	0.857553	0.609974	0.686076	0.875328	0.861013	**0.889278**
LoLI 8	0.819572	0.819145	0.587564	0.685087	0.818548	0.832118	**0.857909**
LoLI 9	0.889372	0.865438	0.637651	0.686258	0.888350	0.871942	**0.905081**
LoLI 10	0.871473	0.881323	0.645677	0.684314	0.871427	0.882034	**0.912178**

Table 4. CII values of images shown in Fig. 8

Image	HE	AHE	CLAHE	GAMMA	IFI	TIFG	TIFG+CLAHE
LoLI 1	1.066912	1.026204	0.480087	0.479728	1.069177	0.824037	**0.878028**
LoLI 2	1.101886	1.017366	0.536962	0.480150	1.102355	0.822182	**0.900365**
LoLI 3	1.046233	1.050401	0.497338	0.469390	1.048598	0.814124	**0.881311**
LoLI 4	1.114559	1.018239	0.524066	0.491002	1.115625	0.839625	**0.912287**
LoLI 5	1.059453	1.014276	0.488126	0.476508	1.060214	0.821204	**0.880800**
LoLI 6	1.044884	1.028541	0.492119	0.469359	1.047728	0.814430	**0.874709**
LoLI 7	1.009383	1.030223	0.494820	0.474242	1.011883	0.821117	**0.882554**
LoLI 8	0.998463	1.015065	0.499717	0.496187	**0.998996**	0.851523	0.908794
LoLI 9	1.104059	1.018564	0.544157	0.476058	1.104972	0.818882	**0.900832**
LoLI 10	1.291848	1.026605	0.551702	0.460428	1.292050	0.801800	**0.903649**

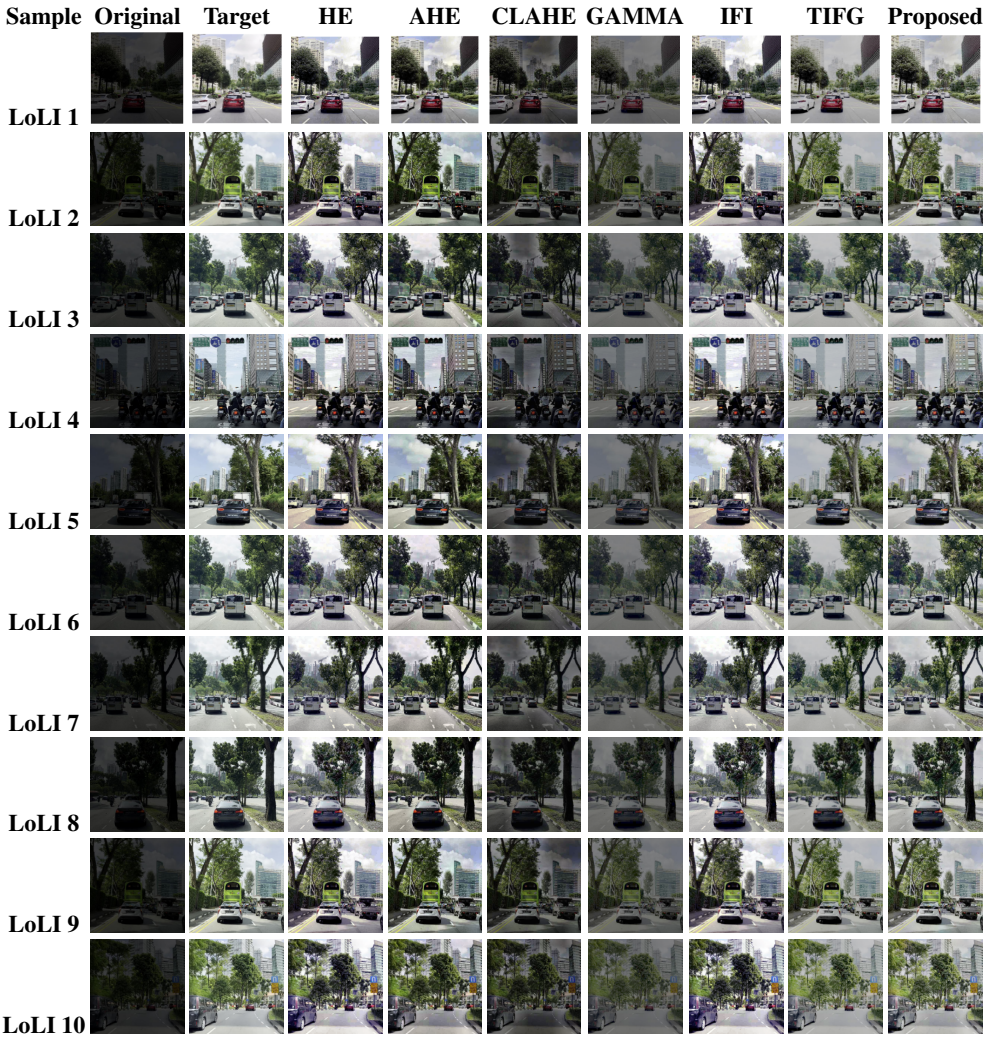

Fig. 8. The comparison of enhanced images from the LoLI-Street datasets [38]. The proposed enhancement method is compared with various existing image enhancement techniques.

fectively enhanced low-light images while preserving brightness, structural details, and visual naturalness. In figure 10 shows the visual comparison of enhanced images from the MIT-5K dataset using various enhancement methods. The proposed enhancement approach provides improved illumination, better contrast enhancement, and consistent brightness preservation compared to conventional techniques, resulting in visually pleasing and structurally preserved outputs.

For quantitative evaluation, Tables 2 - 7 report the results obtained on the LoLI dataset, meanwhile Tables 5 - 7 basically summarize the performance on the ExDark and MIT-5K datasets using the AMBE, SSIM, and CII metrics. Lower AMBE is better for brightness preservation, higher SSIM really means improved structural similarity, and higher CII indicates stronger contrast enhancement.

For the LoLI dataset, the proposed TIFG+CLAHE framework manages to give the lowest AMBE values and the highest SSIM values across most images, demonstrating effective brightness preservation and also retaining the fine structural details. Also, its CII values remain close to the ideal range, suggesting balanced contrast enhancement without noticeable artifacts.

For the ExDark dataset, the standalone TIFG method reaches the lowest AMBE values and SSIM values that are close to 1, so it confirms strong brightness preservation and structural fidelity under challenging low-light conditions. While TIFG produces more natural visual effects, HE and IFI frequently result in over-enhancement despite producing higher CII values.

For the MIT-5K dataset, TIFG+CLAHE obtains superior brightness preservation with lower AMBE values, while still keeping competitive SSIM and also a balanced contrast enhancement. In general, the overall outcomes show that the proposed TIFG and TIFG+CLAHE frameworks enhance low-light images by keeping the brightness cues, preserving structural information, and delivering contrast that looks visually pleasant across the different datasets.

(b) **Computational Efficiency**:

The computational efficiency of the proposed framework was evaluated using execution time and model complexity. The fuzzy

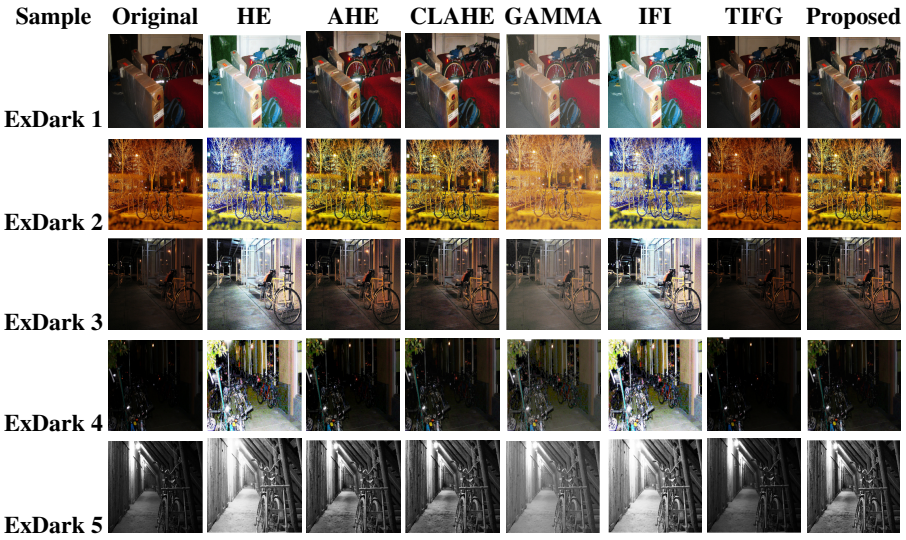

Fig. 9. The Visual comparison of enhanced images from the ExDark Dataset [39]. The proposed enhancement method is compared with various existing image enhancement techniques.

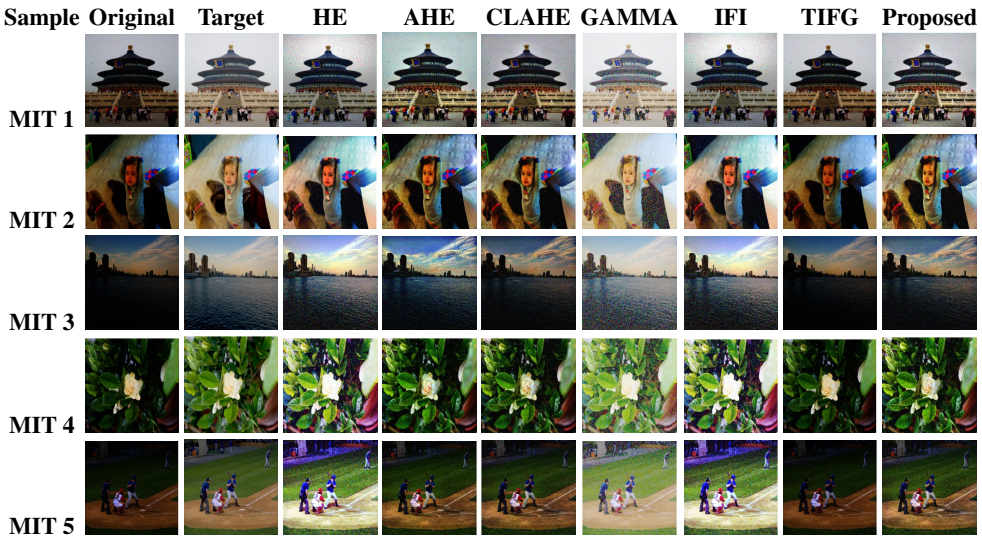

Fig. 10. The visual comparison of enhanced images from the MIT-5K Dataset [40]. The proposed enhancement method is compared with various existing image enhancement techniques.

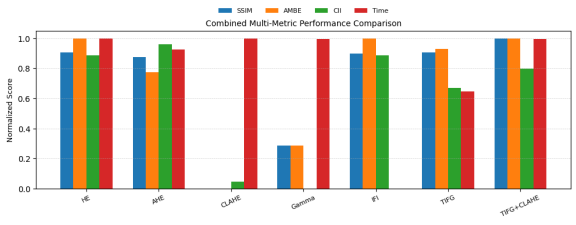

Fig. 11. Performance comparison of different enhancement methods

Table 5. AMBE values of images shown in Fig. 9 and 10

Image	HE	AHE	CLAHE	GAMMA	IFI	TIFG	TIFG+CLAHE
ExDark 1	0.349519	0.077244	0.087426	0.268645	0.349629	**0.011005**	0.077515
ExDark 2	0.231993	0.123285	0.123159	0.268882	0.232721	**0.028973**	0.100018
ExDark 3	0.411737	0.094685	0.107466	0.263257	0.411739	**0.013138**	0.087101
ExDark 4	0.428224	0.038630	0.060733	0.178963	0.428225	**0.008396**	0.042826
ExDark 5	0.312415	0.103603	0.110370	0.270668	0.312612	**0.003643**	0.113049
MIT 1	0.11859	0.12306	0.17229	0.08590	0.59373	0.16366	**0.08198**
MIT 2	**0.07098**	0.19816	0.18808	0.10979	0.50535	0.21280	0.12530
MIT 3	**0.03315**	0.11283	0.18002	0.10258	0.37827	0.21754	0.13748
MIT 4	0.10221	0.09577	0.09382	**0.04163**	0.32228	0.15939	0.04911
MIT 5	0.15612	0.11942	0.10997	**0.04256**	0.30468	0.18756	0.07103

membership network is lightweight, containing only four trainable parameters, which enables fast convergence and low computational overhead during training. Across the ExDark dataset, the proposed TIFG method showed an average processing time of 126.51 ms per image while still keeping a superior enhancement quality. Compared with conventional fuzzy-based approaches

Table 6. SSIM values of images shown in Fig. 9 and 10

Image	HE	AHE	CLAHE	GAMMA	IFI	TIFG	TIFG+CLAHE
ExDark 1	0.371551	0.751253	0.716636	0.500269	0.371392	**0.996974**	0.743497
ExDark 2	0.504730	0.719086	0.693932	0.580519	0.503782	**0.988020**	0.749135
ExDark 3	0.164959	0.636136	0.583705	0.391418	0.164960	**0.988959**	0.662255
ExDark 4	0.053363	0.731019	0.514100	0.196408	0.053364	**0.981205**	0.646839
ExDark 5	0.411590	0.674930	0.657898	0.540045	0.412584	**0.999011**	0.653947
MIT 1	0.5250	0.4817	0.4928	**0.7962**	0.0041	0.6646	0.5508
MIT 2	0.5611	0.4192	0.4215	**0.6371**	0.0476	0.5263	0.4370
MIT 3	0.3839	0.2697	0.2986	**0.5032**	0.0108	0.3282	0.3124
MIT 4	0.4602	0.5279	0.5384	**0.6178**	0.0756	0.4743	0.5517
MIT 5	0.2666	0.4144	0.4335	**0.5363**	0.0103	0.3830	0.4199

Table 7. CII values of images shown in Fig. 9 and 10

Image	HE	AHE	CLAHE	GAMMA	IFI	TIFG	TIFG+CLAHE
ExDark 1	1.872231	1.316066	1.303574	1.139786	1.873393	**0.962019**	1.271154
ExDark 2	1.793314	1.581284	1.538160	0.956737	1.796697	**0.944039**	1.482586
ExDark 3	3.554484	1.803827	1.781626	1.507251	3.554526	**0.923462**	1.664211
ExDark 4	4.149995	1.550694	1.561041	1.858579	4.150009	**0.922896**	1.406314
ExDark 5	1.471963	1.143565	1.124094	**0.949961**	1.473650	1.007044	1.133666
MIT 1	1.1702	1.1273	**0.9819**	1.0874	0.0024	1.2138	1.0917
MIT 2	1.1255	0.8336	0.8313	**0.9134**	0.0008	0.8898	0.9293
MIT 3	1.3241	**1.0332**	0.7740	0.9073	0.0007	0.7550	0.8792
MIT 4	1.3681	1.0289	**0.9966**	0.9716	0.0010	0.9143	1.0840
MIT 5	2.0552	1.0299	**1.0116**	0.9677	0.0013	0.7412	1.1364

like IFI, the proposed framework needs much less computational cost while also giving better quantitative and visual results. Overall, these observations show that the proposed TIFG, and also TIFG+CLAHE frameworks provide an effective balance between enhancement performance and computational efficiency, making them suitable for practical low-light image enhancement applications.

(c) **Qualitative Performance**:
The qualitative performance of the proposed framework was assessed through visual comparisons on the LoLI, ExDark, and MIT-5K datasets, as shown in table 2 - 7. The enhanced images from TIFG and TIFG+CLAHE exhibit improved illumination, enhanced visibility of dark regions, and better contrast while natural colors and fine structures stay largely intact. In contrast, HE, AHE, CLAHE, Gamma correction, and IFI can lead to over-enhancement, brightness shift, or detail loss. The proposed methods instead produce outputs that feel visually balanced with only minor artifacts. These visual outcomes also indicate that the proposed framework improves image quality while keeping brightness consistency and structural fidelity across various low-light imaging conditions.

6. CONCLUSION

This study presented a TIFG+CLAHE approach that combines the characteristics of intuitionistic fuzzy sets with data-driven optimization techniques along with the TIFG-based low-light image enhancement. The TIFG model effectively handles illumination uncertainty through adaptive membership, non-membership, and hesitation components, while the composite loss function ensures reconstruction accuracy, fuzzy consistency, and natural visual appearance. The proposed framework was evaluated on the LoLI, ExDark, and MIT-5K datasets using quantitative and qualitative measures. The results showed superior performance over HE, AHE, CLAHE, Gamma correction, and IFI in terms of AMBE, SSIM, and CII. The standalone TIFG model performed best on the ExDark dataset, while TIFG+CLAHE achieved the most balanced results on the LoLI and MIT-5K datasets. Moreover, its lightweight architecture and moderate execution time demonstrate better computational efficiency. Overall, the proposed TIFG and TIFG+CLAHE methods effectively enhance low-light images by improving visibility, preserving structural details, and maintaining brightness consistency. Future work will focus on developing real-time video enhancement techniques that can maintain temporal consistency between consecutive frames. Further efforts will also aim to improve the robustness of the model under extremely low-light and noisy conditions.

7. REFERENCES

[1] Li, C., Guo, C., Han, L., Jiang, J., Cheng, M.M., Gu, J. and Loy, C.C., 2021. Low-light image and video enhancement using deep learning: A survey. IEEE transactions on pattern analysis and machine intelligence, 44(12), pp.9396-9416.

[2] Lin, Q., Zheng, Z. and Jia, X., 2022. UHD low-light image enhancement via interpretable bilateral learning. Information Sciences, 608, pp.1401-1415.

[3] Wang, W., Chen, Z., Yuan, X. and Wu, X., 2019. Adaptive image enhancement method for correcting low-illumination images. Information Sciences, 496, pp.25-41.

[4] Zadeh, L.A., 1965. Fuzzy sets. Information and control, 8(3), pp.338-353.

[5] Atanassov, K.T., 1999. Intuitionistic fuzzy sets. In Intuitionistic fuzzy sets: theory and applications (pp. 1-137). Heidelberg: Physica-Verlag HD.

[6] Burillo, P. and Bustince, H., 1996. Entropy on intuitionistic fuzzy sets and on interval-valued fuzzy sets. Fuzzy sets and systems, 78(3), pp.305-316.

[7] Hanmandlu, M. and Jha, D., 2006. An optimal fuzzy system for color image enhancement. IEEE Transactions on image processing, 15(10), pp.2956-2966.

[8] Raju, G. and Nair, M.S., 2014. A fast and efficient color image enhancement method based on fuzzy-logic and histogram. AEU-International Journal of electronics and communications, 68(3), pp.237-243.

[9] Kaur, T. and Sidhu, R.K., 2015. Performance evaluation of fuzzy and histogram based color image enhancement. Procedia Computer Science, 58, pp.470-477.

[10] Abubakar, F.M., 2012. Image enhancement using histogram equalization and spatial filtering. International Journal of Science and Research (IJSR), 1(3), pp.105-107.

[11] Kim, Y.T., 1997. Contrast enhancement using brightness preserving bi-histogram equalization. IEEE transactions on Consumer Electronics, 43(1), pp.1-8.

[12] Chen, S.D. and Ramli, A.R., 2003. Minimum mean brightness error bi-histogram equalization in contrast enhancement. IEEE transactions on Consumer Electronics, 49(4), pp.1310-1319.

[13] Ibrahim, H. and Kong, N.S.P., 2007. Brightness preserving dynamic histogram equalization for image contrast enhancement. IEEE Transactions on Consumer Electronics, 53(4), pp.1752-1758.

[14] Kapoor, K. and Arora, S., 2015. Colour image enhancement based on histogram equalization. Electrical & Computer Engineering: An International Journal, 4(3), pp.73-82.

[15] Chen, S.D. and Ramli, A.R., 2004. Preserving brightness in histogram equalization based contrast enhancement techniques. Digital Signal Processing, 14(5), pp.413-428.

[16] Jiang, G., Lin, S.C.F., Wong, C.Y., Rahman, M.A., Ren, T.R., Kwok, N., Shi, H., Yu, Y.H. and Wu, T., 2015. Color image enhancement with brightness preservation using a histogram specification approach. Optik, 126(24), pp.5656-5664.

[17] Pizer, S.M., Amburn, E.P., Austin, J.D., Cromartie, R., Geselowitz, A., Greer, T., ter Haar Romeny, B., Zimmerman, J.B. and Zuiderveld, K., 1987. Adaptive histogram equalization and its variations. Computer vision, graphics, and image processing, 39(3), pp.355-368.

[18] Pisano, E.D., Zong, S., Hemminger, B.M., DeLuca, M., Johnston, R.E., Muller, K., Braeuning, M.P. and Pizer, S.M., 1998. Contrast limited adaptive histogram equalization image processing to improve the detection of simulated spiculations in dense mammograms. Journal of Digital imaging, 11(4), p.193.

[19] Chang, Y., Jung, C., Ke, P., Song, H. and Hwang, J., 2018. Automatic contrast-limited adaptive histogram equalization with dual gamma correction. Ieee Access, 6, pp.11782-11792.

[20] Yadav, G., Maheshwari, S. and Agarwal, A., 2014, September. Contrast limited adaptive histogram equalization based enhancement for real time video system. In 2014 international conference on advances in computing, communications and informatics (ICACCI) (pp. 2392-2397). IEEE.

[21] Chaira, T., 2020. Intuitionistic fuzzy approach for enhancement of low contrast mammogram images. International Journal of Imaging Systems and Technology, 30(4), pp.1162-1172.

[22] Chaira, T., 2021. An intuitionistic fuzzy clustering approach for detection of abnormal regions in mammogram images. Journal of Digital Imaging, 34(2), pp.428-439.

[23] Jebadass, J.R. and Balasubramaniam, P., 2022. Low light enhancement algorithm for color images using intuitionistic fuzzy sets with histogram equalization. Multimedia Tools and Applications, 81(6), pp.8093-8106.

[24] Jebadass, J.R. and Balasubramaniam, P., 2022. Low contrast enhancement technique for color images using interval-valued intuitionistic fuzzy sets with contrast limited adaptive histogram equalization. Soft Computing, 26(10), pp.4949-4960.

[25] Chen, C., Chen, Q., Xu, J. and Koltun, V., 2018. Learning to see in the dark. In Proceedings of the IEEE conference on computer vision and pattern recognition (pp. 3291-3300).

[26] Guo, C., Li, C., Guo, J., Loy, C.C., Hou, J., Kwong, S. and Cong, R., 2020. Zero-reference deep curve estimation for low-light image enhancement. In Proceedings of the IEEE/CVF conference on computer vision and pattern recognition (pp. 1780-1789).

[27] Jiang, Y., Gong, X., Liu, D., Cheng, Y., Fang, C., Shen, X., Yang, J., Zhou, P. and Wang, Z., 2021. Enlightengan: Deep light enhancement without paired supervision. IEEE transactions on image processing, 30, pp.2340-2349.

[28] Lore, K.G., Akintayo, A. and Sarkar, S., 2017. LLNet: A deep autoencoder approach to natural low-light image enhancement. Pattern Recognition, 61, pp.650-662.

[29] Wei, C., Wang, W., Yang, W. and Liu, J., 2018. Deep retinex decomposition for low-light enhancement. arXiv preprint arXiv:1808.04560.

[30] Zhang, Z., Jiang, Y., Jiang, J., Wang, X., Luo, P. and Gu, J., 2021. Star: A structure-aware lightweight transformer for real-time image enhancement. In Proceedings of the IEEE/CVF International Conference on Computer Vision (pp. 4106-4115).

[31] Zadeh, L.A., 1973. Outline of a new approach to the analysis of complex systems and decision processes. IEEE Transactions on systems, Man, and Cybernetics, (1), pp.28-44.

[32] Atanassov, K.T., 1999. Intuitionistic fuzzy sets. In Intuitionistic fuzzy sets: theory and applications (pp. 1-137). Heidelberg: Physica-Verlag HD.

[33] Yager, R.R., 1980. On the measure of fuzziness and negation. II. Lattices. Information and control, 44(3), pp.236-260.

[34] Sugeno, M., 1993. FUZZY MEASURES AND FUZZY INTEGRALS-A SURVEY. Readings in Fuzzy Sets for Intelligent Systems, 251-257.

[35] Yadav, G., Maheshwari, S. and Agarwal, A., 2014, September. Contrast limited adaptive histogram equalization based enhancement for real time video system. In 2014 international conference on advances in computing, communications and informatics (ICACCI) (pp. 2392-2397). IEEE.

[36] Pal, S.K. and King, R., 1981. Image enhancement using smoothing with fuzzy sets. IEEE TRANS. SYS., MAN, AND CYBER., 11(7), pp.494-500.

[37] Palanisami, D., Mohan, N. and Ganeshkumar, L., 2022. A new approach of multi-modal medical image fusion using intuitionistic fuzzy set. Biomedical Signal Processing and Control, 77, p.103762.

[38] Islam, M.T., Alam, I., Woo, S.S., Anwar, S., Lee, I.K. and Muhammad, K., 2024. Loli-street: Benchmarking low-light image enhancement and beyond. In Proceedings of the Asian Conference on Computer Vision (pp. 1250-1267).

[39] Loh, Y.P. and Chan, C.S., 2019. Getting to know low-light images with the exclusively dark dataset. Computer vision and image understanding, 178, pp.30-42.

[40] Shen, L., Yue, Z., Feng, F., Chen, Q., Liu, S. and Ma, J., 2017. Msr-net: Low-light image enhancement using deep convolutional network. arXiv preprint arXiv:1711.02488.

[41] Gupta, B. and Tiwari, M., 2016. Minimum mean brightness error contrast enhancement of color images using adaptive gamma correction with color preserving framework. Optik, 127(4), pp.1671-1676.

[42] Mittal, P., Saini, R.K. and Jain, N.K., 2019. Image enhancement using fuzzy logic techniques. In Soft computing: theories and applications (pp. 537-546). Springer, Singapore.